

METAL-ORGANIC CHEMICALLY VAPOR DEPOSITED YTTRIA-STABILIZED ZIRCONIA (YSZ) FOR THERMAL BARRIER COATINGS

V. G. Varanasi and T. M. Besmann
Oak Ridge National Laboratory
P.O. Box 2008
Oak Ridge, TN 37831-6063

W. Xu and T. L. Starr
University of Louisville
Louisville, KY 40292

INTRODUCTION

Yttria-stabilized zirconia (YSZ) is used as a thermal barrier coating (TBC) to protect super-alloy blades such as Mar-M247 or Rene-N5 during engine operation. The current method for YSZ fabrication for TBC applications is by air-plasma spraying (APS) or electron beam-physical vapor deposition (EB-PVD).¹⁻⁵ APS gives reasonable deposition rates, but has a limited life and aging effects due to its porous and lamellar structure. The EB-PVD coatings are more stable and can accommodate thermomechanical stresses due to their characteristic strain-tolerant, columnar microstructure. EB-PVD, however, is primarily line-of-sight, which often leaves “hidden areas” uncoated, has low throughput, and has high capital cost. The process of metal-organic chemical vapor deposition (MOCVD) is investigated here as an economical alternative to EB-PVD and APS, with the potential for better overall coverage as well as the ability to produce thick (100-250 μm), strain-tolerant, columnar coatings.

MOCVD of YSZ involves the use of zirconium and yttrium organometallic precursors reacting with an oxygen source. Previous researchers have used β -diketonate or chloride precursors and oxygen.⁶⁻⁸ These precursors have low transport rates due to their low carrier solvent solubility.⁹ Solvated zirconium and yttrium butoxide precursors were investigated here due to their higher vapor pressures and high solvent solubility. This work uses previously performed predictive equilibrium modeling and experiments involving butoxide precursors for tetragonal YSZ fabrication.¹⁰

DISCUSSION OF CURRENT ACTIVITIES

From the equilibrium analysis a minimum of 18 moles per minute of molecular oxygen is required for every mole per minute of Y-butoxide + Zr-butoxide ($\text{O}/(\text{Y}+\text{Zr})=35$) to ensure

formation of tetragonal YSZ at 950°C. To assure full oxidation, the oxygen flow rate was selected to be twice the minimum, $O/(Y+Zr)=72$.

YSZ was deposited in the MOCVD reactor shown in Fig. 1. Substrates included alpha-alumina (99.6 % purity: Coors) and a FeCrAlY. The precursors were Y- and Zr-tert butoxides dissolved in toluene and n-butanol, respectively. The precursors were pre-solvated and their solubility was 0.5 M Y in toluene and 2.23 M Zr in n-butanol. From the as-delivered batches, the reactants were mixed together based on their solubility and the desired coating composition. The solution was delivered continuously by a syringe pump through a poppet-seal relief valve into the deposition chamber. To ensure efficient vaporization, the solution was then misted using an ultrasonic atomizer. The misted solution was carried by 300°C O₂ at 1200 sccm to the substrate through a stainless-steel stagnation flow nozzle. The substrate was inductively heated using a Mar-M247 susceptor. The CVD chamber wall and susceptor holder were made of fused silica glass. A thermocouple was placed within the susceptor to control the susceptor temperature, while the substrate temperature was read using an optical pyrometer. Samples were analyzed using X-ray diffraction (XRD) to identify the phases. Scanning electron microscopy (SEM) revealed coating thickness and microstructure. In addition, electron probe microanalysis (EPMA) was used to determine the relative homogeneity of yttrium and zirconium throughout the as-deposited coating.

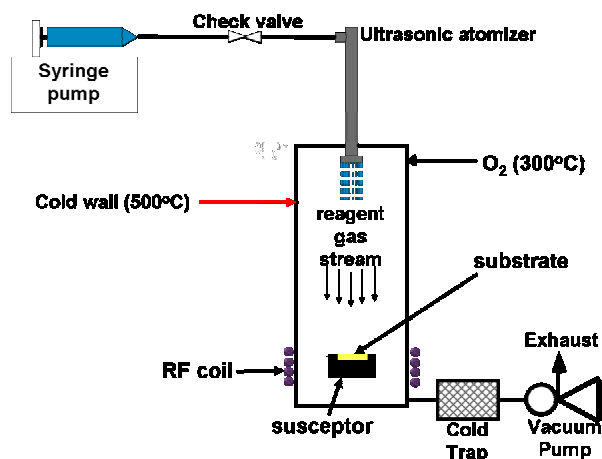


Fig. 1. Schematic of MOCVD system.

Deposition rate as measured from images of the cross-sections vs. substrate temperature is shown in Fig. 2. These agreed well with simple weight gain measurements, where the thickness was calculated from the density of YSZ and the exposed substrate surface area (only the top surface is coated). Coatings up to ~75 μm thick, limited only by the charge to the syringe, were deposited at the higher temperatures. An activation energy assuming an Arrhenius dependence and first order kinetics between 840 and 975°C was calculated to be 53.8 ± 0.2 kJ/mol.

A secondary electron image of a cross-section of the coating on an alumina substrate is presented in Fig. 3, and displays a typical CVD columnar structure. The microprobe images for yttrium

and zirconium signals are also shown, and the non-uniformity, i.e., banding, corresponded to the difference in gray-scale seen in the secondary electron image. In order to further characterize composition, quantitative microprobe measurements were made as a function of position on the cross-section and are shown in Fig. 4. The variation in yttrium and zirconium content is apparent, and the average yttrium proportion was less than half that of the inlet solution. Results of XRD of the coatings indicated a major tetragonal YSZ phase and a minor monoclinic phase.

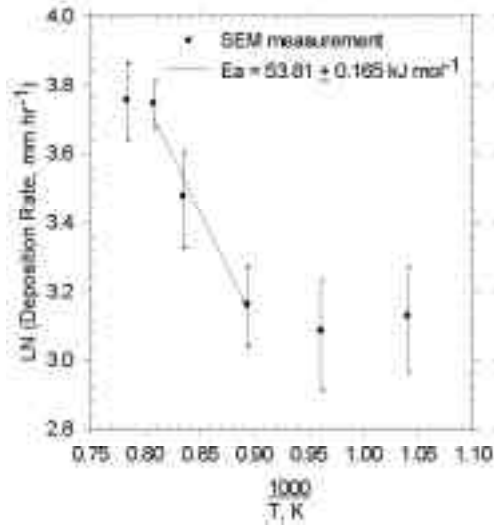


Fig. 2. Arrhenius plot of deposition rates vs. temperature.

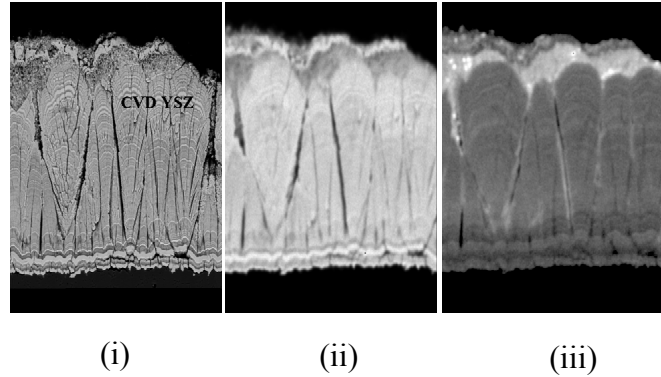


Fig. 3. (i) Secondary electron image, (ii) Zr concentration, and (iii) Y concentration of polished coating cross-section. Coating is $\sim 50 \mu\text{m}$ thick.

Results of initial thermal cycling tests of YSZ-coated FeCrAlY samples are presented in Fig. 4. The uncoated sample experienced slow oxide scale growth, which resulted in small weight gains. A YSZ-coated FeCrAlY sample, on which no polishing or pre-oxidation was performed before coating, suffered substantial weight loss over the thermal cycling period due to severe spallation of the coating. A second substrate with a polished surface that was pre-oxidized in 1 kPa oxygen at 1000°C for 1 h prior to coating to form the desired alumina surface oxide performed significantly better, with minimal weight loss to almost 300 cycles so far (Fig. 5).

Deposition of YSZ with little to no carbon co-deposition is demonstrated under the current conditions. Samples are white in appearance and calcining at 1000°C for several hours yielded minimal to no weight change. The deposition rate dependence on temperature (Fig. 3) appears to indicate a chemical kinetic rate-limiting regime, at least between 840 and 975°C, where the activation energy is relatively large. At higher temperatures, as is typically the case for CVD processing, the chemical kinetic rate becomes more rapid than mass transport to the substrate surface, and thus the apparent activation energy is significantly smaller. The weak temperature dependence behavior observed at low temperatures may be due to complex formation, or failure to form species that would allow efficient oxide deposition.

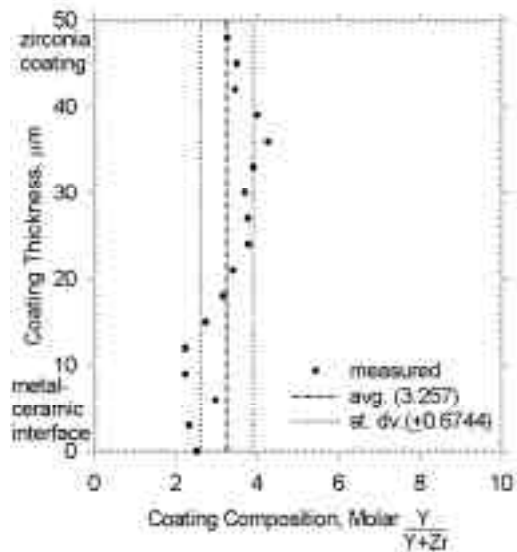


Fig. 4. Yttrium molar ratio as a function of position in a cross-section of a coating.

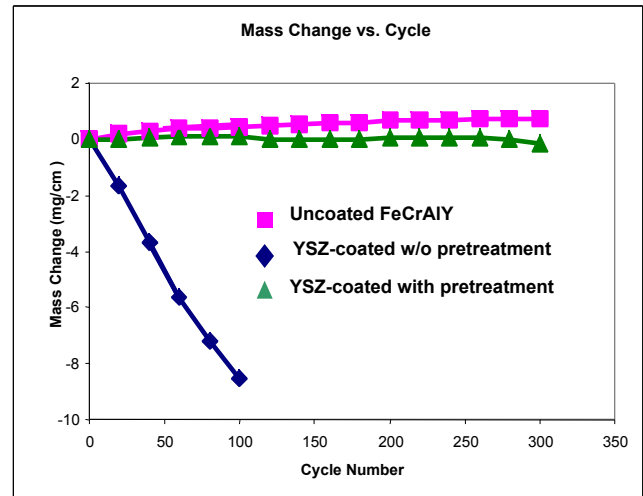


Fig. 5. Mass change as a function of thermal cycles

The non-uniformity in Y:Zr ratio is due to inconsistent precursor delivery or cyclic mass transport issues. The low yttria content of the coatings may have been the result of the recognized greater difficulty in oxidizing yttrium, as compared to zirconium precursors,^{11,12} causing formation of tetragonal coatings with minor monoclinic phase content, as one would expect from the phase equilibria.¹³ Despite the two-phase nature, a YSZ-coated FeCrAlY sample with a pre-oxidized surface exhibited excellent initial thermal cycling behavior.

REFERENCES

1. J. R. Nicholls, "Advances in Coating Design for High-Performance Gas Turbines," *MRS Bull.*, **28** 659-670 (2003).
2. D. R. Clarke and C. G. Levi, "Materials Design for the Next Generation Thermal Barrier Coatings," *Annu. Rev. Mater. Res.*, **33** 383-417 (2003).
3. A. G. Evans, D. R. Mumm, J. W. Hutchinson, G. H. Meier and F. S. Pettit, "Mechanisms Controlling the Durability of Thermal Barrier Coatings", *Progr. Mat. Sci.*, **46** 505-553 (2001).
4. N. P. Padture, M. Gell and E. H. Jordan, "Thermal Barrier Coatings for Gas-Turbine Engine Applications", *Science*, **296** 280-284 (2002).
5. P. K. Wright and A. G. Evans, "Mechanisms Governing the Performance of Thermal Barrier Coatings" *Curr. Opin. Sol. State Phys.*, **4** 255-65 (1999).

6. G. W. Wahl, W. Nemetz, M. Giannozzi, S. Rushworth, D. Baxter, N. Archer, F. Cernuschi, and N. Boyle "Chemical Vapor Deposition of TBC: An Alternative Process for Gas Turbine Components," *Transactions of the ASME*, **123** 520-4 (2001).
7. G. Wahl, Ch. Metz, and S. Samoilenkov "Thermal Barrier Coatings," in Proceedings: Thirteenth European Conference on Chemical Vapor Deposition, EDP Sciences, Les Ulis, France, 2001, pp. Pr3-835-46.
8. H. Yamane and T. Hirai. "Yttria Stabilized Zirconia Transparent Films Prepared by Chemical Vapor Deposition." *Journal of Crystal Growth*, **94** 880-4 (1989).
9. V. G. Varanasi, , T. M. Besmann, (2003). "Parametric Study of the Chemical Vapor Deposition of Yttria-Stabilized Zirconia From Organometallic Precursors," in Proceedings of the Electrochemical Society: Chemical Vapor Deposition XVI and EuroCVD 14, Vol. 2, The Electrochemical Society, Pennington, NJ, 2003, pp. 783-9.
10. V. G. Varanasi, T. M. Besmann, T. L. Starr, W. Xu, and T. J. Anderson, "Yttria-Stabilized Zirconia Thermal Barrier Coatings by Metal-Organic Chemical Vapor Deposition," Proc. High Temperature Ceramic Matrix Composites V, in press.
11. C. Dubourdieu, S.B. Kang, Y.Q. Li, G. Kulesha, B. Gallois, "Solid Single-Spurce Metal Organic Chemical Vapor Deposition of Yttria-Stabilized Zirconia," *Thin Solid Films*, **339** 165-73 (1999).
12. H. Holschuh and H. Sur, "Textured (100) Yttria-Stabilized Zirconia Thin Films Deposited by Plasma-Enhanced Chemical Vapor Deposition," *Appl. Phys. Lett.*, **59** 470-2 (1991).
13. Y. Du and Z. P. Jin, "Thermodynamic Calculation of the ZrO_2 - $YO_{1.5}$ -CaO Phase Diagram." *CALPHAD*, **16** (4) 355-62 (1992).